

# MR Imaging of Convective Delivery of Gadolinium-labeled Liposomes in Rat and Monkey

T. R. McKnight<sup>1</sup>, P. R. Jackson<sup>1</sup>, R. Saito<sup>2</sup>, J. R. Bringas<sup>2</sup>, C. Mamot<sup>3</sup>, E. Proctor<sup>1</sup>, M. S. Berger<sup>2</sup>, J. Park<sup>3,4</sup>, K. Bankiewicz<sup>2</sup>

<sup>1</sup>Department of Radiology, University of California, San Francisco, San Francisco, CA, United States, <sup>2</sup>Department of Neurological Surgery, University of California, San Francisco, San Francisco, CA, United States, <sup>3</sup>Division of Hematology-Oncology, University of California, San Francisco, San Francisco, CA, United States, <sup>4</sup>Hermes Biosciences, Inc., South San Francisco, CA, United States

## Introduction

Convection enhanced delivery (CED) of therapeutic agents is currently being investigated as a method for treating patients with intracranial tumors<sup>1</sup>. With CED, the tumor is directly infused with the agent thereby bypassing the blood-brain barrier, the primary restriction for systemic delivery methods. Recently, liposomes have gained popularity as vehicles for chemotherapeutic agents due to the ability to label them with molecules useful for targeting and/or visualizing the delivery of the drug. We are currently investigating the feasibility of combining the strengths of the two techniques for real-time visualization of drug delivery<sup>2,3</sup>. In this study, the distribution of gadolinium (Gd)-labeled liposomes infused into the brains of rats was imaged with MRI and compared with histology. We then tested the ability to use MRI to monitor the dynamics of liposomal infusion into the brain of a primate. The results of this study demonstrate the accuracy of quantifying infused liposomal volumes with MRI and the ability to visualize the infusion in real-time.

## Methods

**MR Imaging of Rats.** Infusion cannula were used to administer 5, 10, 20, or 40  $\mu\text{L}$  volumes of liposomes encapsulating Gd and the fluorescent indicator DiI-DS to the striatum in either hemisphere of normal Sprague-Dawley rats. All infusions began at a rate of 0.2  $\mu\text{L}/\text{min}$  for 15min followed by .5 and .8  $\mu\text{L}/\text{min}$  infusions for various times depending on the maximum infusion volume<sup>2</sup>. Two to four hours later the rats were anesthetized and placed in a plastic tray with an adjustable bite bar. The tray was placed in a pelvic phased-array coil on a 1.5T GE Signa scanner and coronal T1-weighted 3D SPGRs were acquired with TR/TE/flip = 40 ms/6 ms/30°, 3 NEX, matrix=256x192 and 1 mm slice thickness. The FOV varied from 16 cm to 28 cm, based on the sizes and number of rats imaged at one time.

**Dynamic Imaging of Primates.** Guide cannula to the corpus callosum (CC), corona radiata (CR), and brain stem (BS) were surgically inserted into the skull of a normal rhesus macaque as previously described<sup>4</sup>. The monkey was anesthetized and placed in an MR-compatible stereotactic frame and a 5-inch circular surface coil was placed on top of the skull. Baseline images were acquired using SPGR at flip angles of 8° and 40° with: TR/TE=28ms/8ms, slice = 1 mm, NEX = 4, matrix = 256x192, FOV=16 cm, voxel size = 0.39mm<sup>3</sup>. Infusion cannula were inserted into the three sites. Infusion rates at all 3 sites were increased in a step-wise fashion from 0.1, 0.2, 0.5, 0.8  $\mu\text{L}/\text{min}$  each for 10min, and then held constant at 1  $\mu\text{L}/\text{min}$  to complete the infusion. SPGRs (40° flip angle) were acquired consecutively until the infusion was complete. Each SPGR acquisition lasted for 12:25 min.

**Data Analysis.** Infusion volumes were calculated from histology (rats) and MR images (rats and primate). For histology, fluorescent images were taken at 1mm intervals using a fluorescent microscope and CCD camera. The distribution of liposomes was quantified using NIH image 1.62 (Bethesda, MD)<sup>2</sup>. For the MR images, background values were obtained from extracranial muscle near the infusion sites. The original MR images were filtered with a Sobel edge detection kernel using IDL (RSI, Boulder, CO). The filtered images were used to create masks of the liposomal distribution boundaries in the brain. After the original images were masked, the liposomal distribution was refined using a threshold that was based on the background values.

## Results

**Validation of MRI Volume Analysis in Rats.** Figure 1 shows the correlation between the infusion volumes measured in the histologic sections by fluorescence and those measured in the MRI ( $r = 0.763$ ,  $P = 0.05$  two-tailed t-test). Both measurements showed a 3:1 ratio of MRI distribution volume to infused volume. The variation in voxel sizes (0.12 - 1.19 mm<sup>3</sup>) and signal-to-noise ratios (SNR range 21-115) within the MRIs were two possible sources of error in our measurements. However, neither was correlated with the measured infusion volume suggesting that the error was minimal. This was further supported by, the significant correlation ( $r = 0.82$ ,  $P = 0.02$ ) between the volume of distribution calculated by MRI and the infused volume.

### Real-time Imaging of Liposomal Infusion in Monkey Brain.

Figure 2 shows SPGRs images displaying the step-wise increase in liposomal volume that was observed in the CC

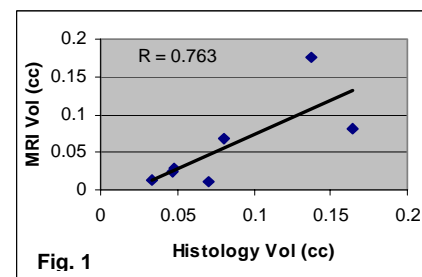
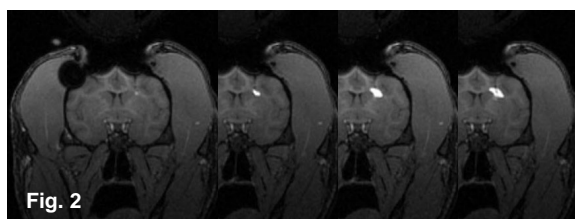


Fig. 1

at baseline and after 22, 45, and 68 min. of infusion. Similar increases were seen in the CR and BS. The loading curves of all three sites were similar, with an initial slope during the step-wise increase in infusion rate and a plateau once the infusion rate became constant. The SNR at the infused sites ranged from 20 – 85 with the lowest occurring at the BS. The smallest volume that could be detected in each region were 12  $\mu\text{L}$ , 10  $\mu\text{L}$ , and 25  $\mu\text{L}$  and had SNRs of 36, 39, and 40 for the CC, CR, and BS respectively. However, the ratios of MRI:infused volumes at those same timepoints were 10:1, 2:1, and 2:1, respectively, suggesting that the liposomes distributed within the CC more readily than at the other sites. This finding warrants further investigation.

## Discussion

We demonstrated the ability to accurately quantify the infused volume of Gd-liposomes in normal rat brain with SPGR MRIs. Thus in a clinical setting, the infusion could be monitored and adjusted to cover the majority of the diseased region while sparing normal tissue. We also performed a single study in primate brain that demonstrated the ability to visualize the CED of Gd-liposomes in real-time. We acquired SPGR images with two different flip angles and sufficient resolution and SNR (based on the rat studies) to quantify the temporal changes in the gadolinium concentration profiles at three infusion sites. Although the adjustments made to the infusion scheme during the real-time experiment prevented accurate quantification of the distribution parameters, the feasibility of using MRI to monitor CED of Gd-liposomes in a model that more closely the human condition was demonstrated. More experiments are needed to verify the accuracy of quantifying the MRI distributions in real-time as well as to assess the reproducibility of the loading characteristics within specific brain regions.

## Acknowledgements

David Newitt, Ph.D., Accelerate Brain Cancer Cure, UCSF Brain Tumor SPORE

## References

1. Kunwar, S. (2003) Convection enhanced delivery of IL13-PE38QQR for treatment of recurrent malignant glioma: presentation of interim findings from ongoing phase I studies. *Acta Neurochir Suppl*, 88, 105-11.
2. Saito, R. et. al. Effective distribution of liposomes into the central nervous system and brain tumor models by convection-enhanced delivery monitored with magnetic resonance imaging. (submitted to *Canc Res*)
3. Mamot, C. et.al., Extensive Distribution of Liposomes in Rodent Brain and Brain Tumors Following Convection Enhanced Delivery (CED) (*J Neuro-onc*, in press).
4. Bankiewicz, K. et.al. (2000) Convection Enhanced Delivery of AAV Vector in Parkinsonian Monkeys; In Vivo Detection of Gene Expression and Restoration of Dopaminergic Function Using Pro-drug Approach. *Experimental Neurology*, 164, 2-14.